

Fig. S1. Raman spectra of (a) MoS_2 and (b) carbon in MoS_2 -only, MoS_2/GNS 9:1, MoS_2/GNS 8:2, and MoS_2/GNS 7:3.

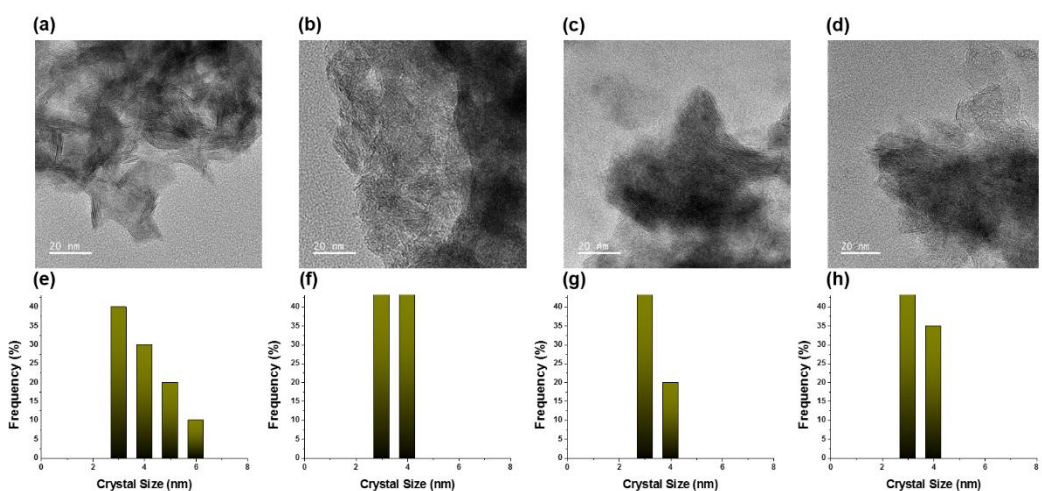


Fig. S2. TEM images and particle size distributions of (a),(e) MoS₂-only, (b),(f) MoS₂/GNS 9:1, (c),(g) MoS₂/GNS 8:2, and (d),(h) MoS₂/GNS 7:3.

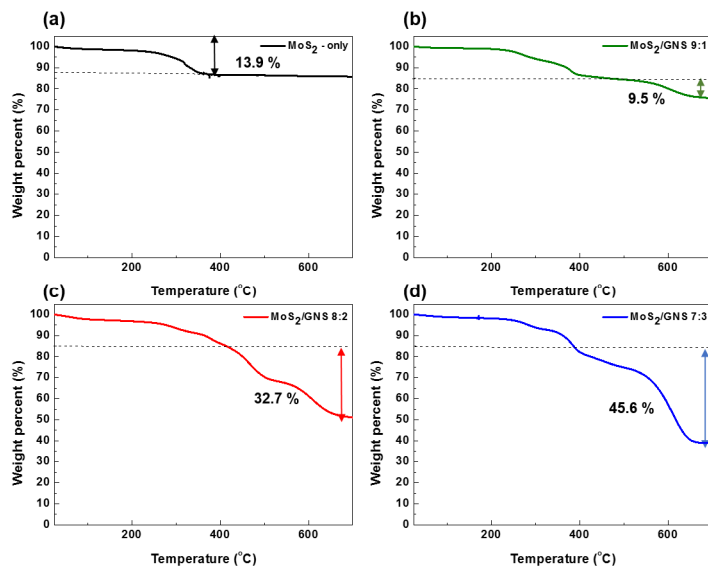


Fig. S3. TGA curves of (a) MoS₂-only, (b) MoS₂/GNS 9:1, (c) MoS₂/GNS 8:2, and (d) MoS₂/GNS 7:3.

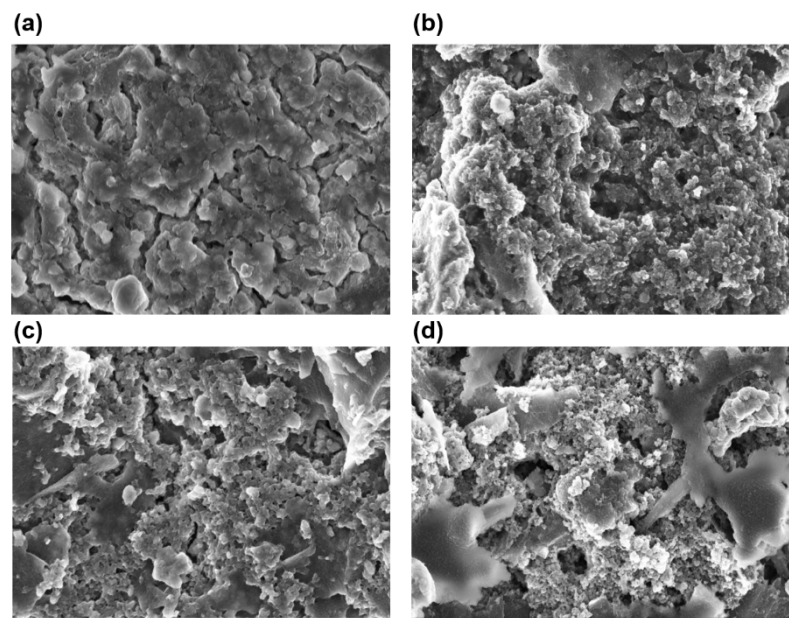


Fig. S4. SEM images of (a) MoS₂-only, (b) MoS₂/GNS 9:1, (c) MoS₂/GNS 8:2, and (d) MoS₂/GNS 7:3 after 100 cycles.

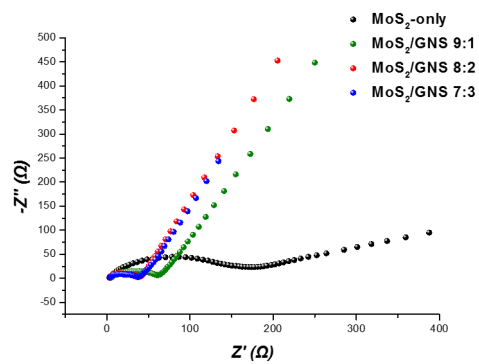


Fig. S5. Nyquist plots of the samples measured at a current of 200 mA g⁻¹ in the initial states.

Table. S1. Comparison of electrochemical performance of MoS₂-based anodes for LIBs

Sample	Current density (mA g ⁻¹)	Capacity (mA g ⁻¹)	Cycle number	Ref
MoS ₂ /GNS	200	613	100	In this work
Hierarchical hollow MoS ₂ nanotubes	100	727	100	8
MoS ₂ /nano-silicon@carbon	100	767.52	250	24
MoS ₂ nanosheet in N-doped carbon	100	747	100	38
Hierarchical MoS ₂ /N-doped carbon nanobelts	100	901	100	35
MoS ₂ and multilayered holey graphene	100	591	10	37
MoS ₂ nanoflakes/N-doped carbon	1000	490	100	36